24th COBEM - 2017

24th ABCM International Congress of Mechanical Engineering
December 3-8, 2017, Curitiba, PR, Brazil

COBEM-2017-1982
BAND GAPS IN PLATES AND CYLINDRICAL SHELLS WITH 1D PERIODIC ELASTIC PROPERTIES

R. W. O. Sousa
University of Campinas - UNICAMP, Computational Mechanics Department, Rua Mendeleyev, 200, CEP13083-860, Campinas, SP, Brazil
raystonsousa@gmail.com

J.-M. Mencik
INSA Centre Val de Loire, Campus de Blois, Rue de la Chocolaterie, 41000 Blois, France
jean-mathieu.mencik@insa-cvl.fr

J. M. C. Dos Santos
University of Campinas - UNICAMP, Computational Mechanics Department, Rua Mendeleyev, 200, CEP13083-860, Campinas, SP, Brazil
zema@fem.unicamp.br

Abstract. *In this work, the wave propagation in phononic crystal plates and cylindrical shells is analyzed. The main purpose is to investigate the properties of the periodicity on the frequency band structure, and especially, the location and width of band gaps. To analyze the phononic crystal systems, a numerical technique called wave finite element (WFE) method is investigated. It uses the concept of transfer matrix methods to calculate the wave propagation behavior along one-dimensional (1D) periodic systems. In this paper, the WFE method is used to calculate band gaps in elastic phononic crystal plates and cylindrical shells with a periodic distribution of different elastic properties. Band gaps generated by Bragg scattering effect are calculated with the WFE method through different test cases. Results are presented in the form of dispersion diagrams and frequency response functions. The relevance of the WFE method is clearly demonstrated in comparison with different analytical theories.*

Keywords: *periodic structures, phononic crystals, band gaps, wave finite element method, spectral element method*

1. INTRODUCTION

Various engineering applications such as marine, automobile, aircraft and civil engineering structures are approximated using plate and shell models. Phononic crystals (PCs) can be seen as composite materials, i.e., structures having different elastic properties which are periodically distributed along their length (see Figure 1). Due to their periodic nature, those structures may exhibit band gaps, i.e., stop bands or forbidden bands over which waves do not propagate. This interesting feature enables one to propose efficient solutions for the vibration and sound insulation of structures.

In the 70's, Mead started working on the propagation of waves along 1D periodic structures, i.e., structures made up of identical substructures along a certain straight or curved direction (Mead, 1970). New methods have since emerged which use periodicity modeling together with numerical modeling to analyze complex structures at a low computational cost. Among these, the WFE method considers the finite element (FE) model of a substructure — i.e., a periodicity pattern — to express a transfer matrix relation. Computing the eigenvalues and eigenvectors of the transfer matrix provides, from Bloch's theorem, the so-called wave modes which travel towards the right and left directions along a periodic structure (Mencik and Ichchou, 2005; Duhamel *et al.*, 2006). The WFE method has been applied to various kinds of structures, e.g., beams, thin plates, cylindrical shells, and also, periodic structures with complex periodicity patterns (Mencik, 2014).

There have been numerous researches in the field of PCs and metamaterials over the last decades. Analyzing and understanding these systems from the computational (modeling) and experimental points of view remains an open challenge however, especially in the engineering field (Hussein *et al.*, 2014). One interesting characteristic of PCs is to produce band gaps. These are mostly induced by Bragg scattering effect, i.e., when impedance mismatches — i.e., changes in the elastic properties — periodically occur along a structure. In fact, band gaps generally appear around frequencies governed by the Bragg condition, i.e., $\Delta = n''(\lambda/2)$ ($n'' = 1, 2, ...$) with λ the wavelength and Δ the space between two consecutive impedance mismatches.

Most of the studies made on PCs have focused on investigating bulk waves. Recently, some studies have been con-

ducted on elastic waves in plates. Most of these work by considering the plane wave expansion (PWE) method along with the Kirchhoff-Love thin plate theory or the Reissner-Mindlin thick plate theory (Hsu and Wu, 2006; Wu *et al.*, 2011). The main issue when using the PWE method is that the structures are assumed to be infinite, i.e., it cannot be applied to analyze the dynamic behavior of systems such as plates of finite dimensions, finite cylindrical shells and so on... that is to say, structures which are frequently encountered in the engineering industry. Another technique to evaluate band gaps in plates and shells has been proposed by Sorokin and Ershova (2004). This provides a means to analyze the formation of band gaps in plates and shells with or without fluid loading using the Floquet-Bloch theory and the boundary integral equation methodology. Finally, Shen *et al.* (2013) have investigated band gaps in fluid-filled cylindrical shells with active and passive control by FE analysis.

In this paper, the WFE method is applied to compute band gaps in simply-supported plates and cylindrical shells whose elastic properties periodically vary as shown in Figure 1. The motivation behind this work is to demonstrate that the WFE method is accurate and efficient for modeling and simulating these kinds of PCs. For this task, a comparative study is proposed between the WFE method and the SE method. The SE method uses an exact analytical solution issued from the Levy-plate theory, while the WFE method uses FE models. Hence, the WFE method is used to analyze the wave propagation in PC structures, and further their forced response. The WFE method can be used to analyze complex periodic structures with arbitrary-shaped periodicity patterns, and as such, it can be applied to systems which cannot be handled with the SE method. This leads the way to interesting prospects for computing band gaps in periodic structures whose shapes can be designed so as to magnify band gap effects.

The rest of the paper is organized as follows. The basics of the WFE method are recalled in Section 2. Here, the so-called $\mathbf{S} + \mathbf{S}^{-1}$ transformation technique is considered to compute the waves in periodic structures with accurate precision. Also, the WFE strategy to compute the forced response of periodic structures is recalled. In Section 3, the SE method for homogeneous and PC Levy-plates is reviewed. Numerical experiments are brought in Section 4 which concern a PC simply-supported plate and a PC cylindrical shell. The relevance of the proposed method to identify the location and width of band gaps in the dispersion curves and frequency response functions is discussed. Comparisons are made with the SE method for plates and the Flügge theory for shells which highlight the accuracy of the numerical predictions.

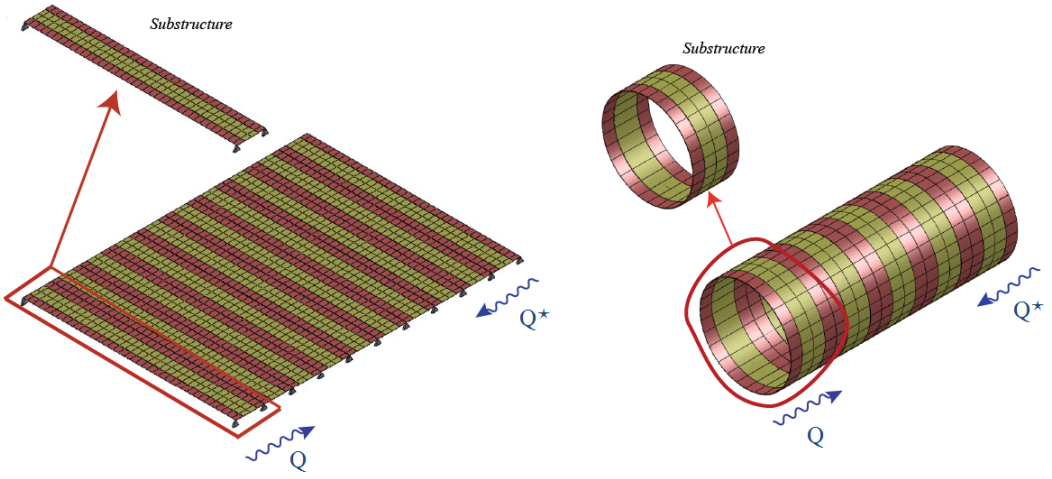

Figure 1: FE mesh of two periodic structures having different elastic properties periodically distributed along their length. (Left) periodic plate; (Right) periodic cylindrical shell.

2. WFE METHOD

2.1 Wave propagation along periodic structures

Consider a periodic structure composed of identical substructures which are made up of strips with different material properties as shown in Figure 1. Within FE framework, it is assumed that the substructures are meshed in the same way with the same number n of degrees of freedom (DOFs) on their left and right boundaries. Hence, the dynamic stiffness matrix of a given substructure can be expressed by

$$\mathbf{D} = -\omega^2\mathbf{M} + (1 + \mathtt{i}\eta)\mathbf{K}, \tag{1}$$

where $\mathbf{M}$ and $\mathbf{K}$ are the mass matrix and stiffness matrix of the substructure, respectively. Also, ω and η are the angular frequency and the loss factor, respectively. The WFE method consists in assessing the so-called wave modes $(\mu_j, \boldsymbol{\phi}_j)$ of the periodic structure. These are the eigensolutions of the following $2n \times 2n$ symplectic matrix $\mathbf{S}$:

$$\mathbf{S} = \begin{bmatrix} -\mathbf{D}_{\mathtt{LR}}^{*-1}\mathbf{D}_{\mathtt{LL}}^{*} & -\mathbf{D}_{\mathtt{LR}}^{*-1} \\ \mathbf{D}_{\mathtt{RL}}^{*} - \mathbf{D}_{\mathtt{RR}}^{*}\mathbf{D}_{\mathtt{LR}}^{*-1}\mathbf{D}_{\mathtt{LL}}^{*} & -\mathbf{D}_{\mathtt{RR}}^{*}\mathbf{D}_{\mathtt{LR}}^{*-1} \end{bmatrix}. \tag{2}$$

The matrix $\mathbf{S}$ is to be understood as the transfer matrix of a substructure, which links the displacement/force vectors between its right and left boundaries. In Eq. (2), $\mathbf{D}^*$ is the dynamic stiffness matrix of the substructure condensed on its left and right boundaries. It is expressed as $\mathbf{D}^* = \mathbf{D}_{\mathtt{BB}} - \mathbf{D}_{\mathtt{BI}}\mathbf{D}_{\mathtt{II}}^{-1}\mathbf{D}_{\mathtt{IB}}$ where subscripts `B` and `I` refer to the boundary DOFs — i.e., those on the left and right boundaries — and the internal DOFs, respectively. It is worth noting that the computation of $\mathbf{D}^*$ can be cumbersome when the number of internal DOFs is high. However, this numerical task can be considerably sped up by considering the Craig-Bampton (CB) method, in the framework of which a reduced sets of fixed-interface modes are considered (see Mencik (2014)).

The wave modes are denoted as $(\mu_j, \boldsymbol{\phi}_j)$ where μ_j and $\boldsymbol{\phi}_j$ refer to the eigenvalues and right eigenvectors of $\mathbf{S}$, respectively. The eigenvalues μ_j are usually referred to as the wave parameters which are expressed by $\mu_j = \mathtt{exp}(-\mathtt{i}\beta_j d)$ where β_j are the wavenumbers, and d is the substructure length. Also, the eigenvectors $\boldsymbol{\phi}_j$ are referred to as the wave shapes which are partitioned into displacement and force vector components, as follows:

$$\boldsymbol{\phi}_j = \begin{bmatrix} \boldsymbol{\phi}_{\mathtt{q}j} \\ \boldsymbol{\phi}_{\mathtt{F}j}, \end{bmatrix} \tag{3}$$

where $\boldsymbol{\phi}_{\mathtt{q}j}$ and $\boldsymbol{\phi}_{\mathtt{F}j}$ are $n \times 1$ vectors of displacement and force components, respectively. Also, due to the fact that the matrix $\mathbf{S}$ is symplectic, its eigenvalues come in pairs as $(\mu_j, 1/\mu_j)$. As it turns out, there exist n right-going wave modes $(\mu_j, \boldsymbol{\phi}_j)$ for which $|\mu_j| < 1$, and n left-going wave modes $(\mu_j^\star, \boldsymbol{\phi}_j^\star)$ where $\mu_j^\star = 1/\mu_j$ and $|\mu_j^\star| > 1$.

2.2 Wave mode computation

The direct computation of the eigensolutions of the matrix S in Eq. (2) is usually prone to numerical ill-conditioning. To solve this issue, an alternative well-conditioned generalized eigenproblem based on the so-called $\mathbf{S} + \mathbf{S}^{-1}$ transformation technique can be considered (see Mencik and Duhamel (2015)). For the sake of clarity, the key steps of this procedure are recalled hereafter.

Within the framework of the $\mathbf{S} + \mathbf{S}^{-1}$ transformation technique, the following generalized eigenproblem is considered with double eigenvalues λ_j of the form $\lambda_j = \mu_j + 1/\mu_j$:

$$\left((\mathbf{N}'\mathbf{J}\mathbf{L}'^T + \mathbf{L}'\mathbf{J}\mathbf{N}'^T) - \lambda_j \mathbf{L}'\mathbf{J}\mathbf{L}'^T \right) \mathbf{z}_j = \mathbf{0}, \tag{4}$$

where

$$\mathbf{L}' = \begin{bmatrix} \mathbf{0} & \mathbf{I}_n \\ \mathbf{D}_{\mathtt{LR}}^{*} & \mathbf{0} \end{bmatrix} \quad , \quad \mathbf{N}' = \begin{bmatrix} \mathbf{D}_{\mathtt{RL}}^{*} & \mathbf{0} \\ -(\mathbf{D}_{\mathtt{LL}}^{*} + \mathbf{D}_{\mathtt{RR}}^{*}) & -\mathbf{I}_n \end{bmatrix} \quad , \quad \mathbf{J} = \begin{bmatrix} \mathbf{0} & \mathbf{I}_n \\ -\mathbf{I}_n & \mathbf{0} \end{bmatrix}, \tag{5}$$

$$\mathbf{N}'\mathbf{J}\mathbf{L}'^T + \mathbf{L}'\mathbf{J}\mathbf{N}'^T = \begin{bmatrix} \mathbf{D}_{\mathtt{RL}}^{*} - \mathbf{D}_{\mathtt{LR}}^{*} & (\mathbf{D}_{\mathtt{LL}}^{*} + \mathbf{D}_{\mathtt{RR}}^{*}) \\ -(\mathbf{D}_{\mathtt{LL}}^{*} + \mathbf{D}_{\mathtt{RR}}^{*}) & \mathbf{D}_{\mathtt{RL}}^{*} - \mathbf{D}_{\mathtt{LR}}^{*} \end{bmatrix}, \tag{6}$$

and

$$\mathbf{L}'\mathbf{J}\mathbf{L}'^T = \mathbf{N}'\mathbf{J}\mathbf{N}'^T = \begin{bmatrix} \mathbf{0} & -\mathbf{D}_{\mathtt{RL}}^{*} \\ \mathbf{D}_{\mathtt{LR}}^{*} & \mathbf{0} \end{bmatrix}. \tag{7}$$

The nice feature of the eigenproblem (4) is that it involves skew-symmetric matrices ($\mathbf{N}'\mathbf{J}\mathbf{L}'^T + \mathbf{L}'\mathbf{J}\mathbf{N}'^T$) and $\mathbf{L}'\mathbf{J}\mathbf{L}'^T$. In this sense, it can be shown that the symplectic nature of the eigenproblem is preserved, i.e., the computed eigenvalues $\lambda_j = \mu_j + 1/\mu_j$ and $\lambda_j^\star = \mu_j^\star + 1/\mu_j^\star$ for the right-going and left-going wave modes will be identical. The eigenvalues $(\mu_j, \mu_j^\star)$ can be found analytically by solving a quadratic equation of the form

$$x^2 - \lambda_j x + 1 = 0, \tag{8}$$

whose solutions are

$$\mu_j, \mu_j^\star = \frac{\lambda_j \pm \sqrt{\lambda_j^2 - 4}}{2}. \tag{9}$$

Finally, the wave shapes $(\boldsymbol{\phi}_j, \boldsymbol{\phi}_j^\star)$ can be retrieved as follows

$$\boldsymbol{\phi}_j = \begin{bmatrix} \mathbf{I}_n & \mathbf{0} \\ \mathbf{D}_{\mathtt{RR}}^* & \mathbf{I}_n \end{bmatrix} \mathbf{w}_j' \quad , \quad \boldsymbol{\phi}_j^\star = \begin{bmatrix} \mathbf{I}_n & \mathbf{0} \\ \mathbf{D}_{\mathtt{RR}}^* & \mathbf{I}_n \end{bmatrix} \mathbf{w}_j'^\star, \tag{10}$$

where

$$\mathbf{w}_j' = \mathbf{J}(\mathbf{L}'^T - \mu_j^\star \mathbf{N}'^T)\mathbf{z}_j \quad , \quad \mathbf{w}_j'^\star = \mathbf{J}(\mathbf{L}'^T - \mu_j \mathbf{N}'^T)\mathbf{z}_j, \tag{11}$$

where $\mathbf{z}_j$ is the eigenvector (eigenproblem (4)) for the eigenvalue λ_j or $\lambda_j^\star$.

2.3 Forced response computation

Consider, for the sake of clarity, a periodic structure composed of N substructures (see Figure 1) whose left side is subjected to a force vector $\mathbf{F}_0$ and whose right side is subjected to prescribed displacements (vector $\mathbf{q}_0$). Within the WFE framework, the displacement vector and force vector on the left and right boundaries of a substructure k ($k = 1, \ldots, N$) are expressed in terms of wave mode shapes, as follows (Mencik, 2014):

$$\mathbf{q}_{\mathtt{L}}^{(k)} = \boldsymbol{\Phi}_{\mathtt{q}} \boldsymbol{\mu}^{k-1} \mathbf{Q} + \boldsymbol{\Phi}_{\mathtt{q}}^\star \boldsymbol{\mu}^{N-k+1} \mathbf{Q}^\star \quad , \quad \mathbf{q}_{\mathtt{R}}^{(k)} = \boldsymbol{\Phi}_{\mathtt{q}} \boldsymbol{\mu}^{k} \mathbf{Q} + \boldsymbol{\Phi}_{\mathtt{q}}^\star \boldsymbol{\mu}^{N-k} \mathbf{Q}^\star, \quad k = 1, \ldots, N, \tag{12}$$

$$-\mathbf{F}_{\mathtt{L}}^{(k)} = \boldsymbol{\Phi}_{\mathtt{F}} \boldsymbol{\mu}^{k-1} \mathbf{Q} + \boldsymbol{\Phi}_{\mathtt{F}}^\star \boldsymbol{\mu}^{N-k+1} \mathbf{Q}^\star \quad , \quad \mathbf{F}_{\mathtt{R}}^{(k)} = \boldsymbol{\Phi}_{\mathtt{F}} \boldsymbol{\mu}^{k} \mathbf{Q} + \boldsymbol{\Phi}_{\mathtt{F}}^\star \boldsymbol{\mu}^{N-k} \mathbf{Q}^\star, \quad k = 1, \ldots, N, \tag{13}$$

where $\boldsymbol{\Phi}_{\mathtt{q}}$, $\boldsymbol{\Phi}_{\mathtt{q}}^\star$, $\boldsymbol{\Phi}_{\mathtt{F}}$ and $\boldsymbol{\Phi}_{\mathtt{F}}^\star$ are $n \times n$ matrices of wave shapes, expressed by

$$\boldsymbol{\Phi}_{\mathtt{q}} = \left[\boldsymbol{\phi}_{\mathtt{q}1} \cdots \boldsymbol{\phi}_{\mathtt{q}n}\right] \quad , \quad \boldsymbol{\Phi}_{\mathtt{q}}{}^\star = \left[\boldsymbol{\phi}_{\mathtt{q}1}^\star \cdots \boldsymbol{\phi}_{\mathtt{q}n}^\star\right], \tag{14}$$

$$\boldsymbol{\Phi}_{\mathtt{F}} = \left[\boldsymbol{\phi}_{\mathtt{F}1} \cdots \boldsymbol{\phi}_{\mathtt{F}n}\right] \quad , \quad \boldsymbol{\Phi}_{\mathtt{F}}{}^\star = \left[\boldsymbol{\phi}_{\mathtt{F}1}^\star \cdots \boldsymbol{\phi}_{\mathtt{F}n}^\star\right]. \tag{15}$$

Also, in Eqs. (12) and (13), $\boldsymbol{\mu}$ is the $n \times n$ diagonal matrix of wave parameters μ_j for the right-going wave modes, i.e., $\boldsymbol{\mu} = \mathtt{diag}\{\mu_j\}_{j=1,\ldots,n}$ where $|\mu_j| < 1$ and $\|\boldsymbol{\mu}\|_2 < 1$. Finally, $\mathbf{Q} = [Q_1 \cdots Q_n]^T$ and $\mathbf{Q}^\star = [Q_1^\star \cdots Q_n^\star]^T$ are $n \times 1$ vectors of wave amplitudes defined at the left and right sides of the whole periodic structure, respectively. By considering Eqs. (12) and (13) as well as the boundary conditions at the left and right sides of the whole structure, a well-conditioned wave-based matrix equation can be expressed as follows:

$$\begin{bmatrix} \mathbf{I}_n & \boldsymbol{\Phi}_{\mathtt{F}}^{-1} \boldsymbol{\Phi}_{\mathtt{F}}^\star \boldsymbol{\mu}^N \\ \boldsymbol{\Phi}_{\mathtt{q}}^{\star -1} \boldsymbol{\Phi}_{\mathtt{q}} \boldsymbol{\mu}^N & \mathbf{I}_n \end{bmatrix} \begin{pmatrix} \mathbf{Q} \\ \mathbf{Q}^\star \end{pmatrix} = \begin{pmatrix} -\boldsymbol{\Phi}_{\mathtt{F}}^{-1} \mathbf{F}_0 \\ \boldsymbol{\Phi}_{\mathtt{q}}^{\star -1} \mathbf{q}_0 \end{pmatrix}. \tag{16}$$

The matrix formulation (16) is of the form $\mathcal{A}\mathcal{Q} = \mathcal{F}$, were $\mathcal{Q} = [\mathbf{Q}^T \, \mathbf{Q}^{\star T}]^T$ and $\mathcal{F}$ stands for the vector of excitations. Solving the matrix equation yields the vectors of wave amplitudes as $\mathcal{Q} = \mathcal{A}^{-1}\mathcal{F}$. The displacement/force vectors at any substructure boundary follow from Eqs. (12) and Eq. (13).

3. SE METHOD FOR LEVY PLATES

The SE method for a Levy-type plate may be derived in analogy with the Kirchhoff-Love plate (Lee and Lee, 1999; Doyle, 1997; Campos and Dos Santos, 2015). In the frequency domain, the governing equation of a Kirchhoff-Love plate is given by (Arruda *et al.*, 2004):

$$D\nabla^2\nabla^2 w(x,y) - \omega^2 \rho h w(x,y) = F(x,y), \tag{17}$$

where $D = Eh^3/12(1-\nu^2)$ is the bending rigidity, h is the thickness, ν is the Poisson ratio, ρ is the density, $w(x,y)$ is the transverse displacement and $F(x,y)$ is the applied surface load. By considering the Levy-plate theory, the transverse displacement of a flat plate which is simply supported along two parallel edges ($x-$direction) is expressed as follows:

$$w(x,y) = \sum_{n=1}^{\infty} \left[\mathbf{A}_n e^{-\mathtt{i}\beta_{1n}x} + \mathbf{B}_n e^{\mathtt{i}\beta_{1n}x} + \mathbf{C}_n e^{-\beta_{2n}x} + \mathbf{D}_n e^{\beta_{2n}x}\right] \mathtt{sin}(\beta_{yn} y), \tag{18}$$

where β_{1n} and β_{2n} are wavenumbers:

$$\beta_{1n} = \sqrt{\beta_p^2 - \beta_{yn}^2} \quad , \quad \beta_{2n} = \sqrt{\beta_p^2 + \beta_{yn}^2}, \tag{19}$$

where

$$\beta_p = (\omega^2 \rho h / D)^{1/4} \quad , \quad \beta_{yn} = \frac{n\pi}{L_y}. \tag{20}$$

The coefficients $\mathbf{A}_n$, $\mathbf{B}_n$, $\mathbf{C}_n$ and $\mathbf{D}_n$ in Eq. (18) are determined from the boundary conditions at the left and right ends of the plate (Arruda *et al.*, 2004). Consider for instance a simply-supported strip of length $d^{\mathtt{s}}$, it becomes possible to link the shearing forces and bending moments on the sides $x = 0$ and $x = d^{\mathtt{s}}$ to the displacements and slopes on the same sides. This yields the dynamic stiffness matrix of the strip (Arruda *et al.*, 2004; Lee and Lee, 1999):

$$\mathbf{D}^{\mathtt{SE}} = [\mathscr{B}]\,[\mathscr{A}]^{-\mathbf{1}}, \tag{21}$$

where

$$\mathscr{B} = D \begin{bmatrix} \alpha_1 & \alpha_1 & \alpha_1 & \alpha_1 \\ \gamma_1 & \gamma_1 & \gamma_2 & \gamma_2 \\ -\alpha_1 e^{-\mathtt{i}\beta_1 d^{\mathtt{s}}} & \alpha_1 e^{\mathtt{i}\beta_1 d^{\mathtt{s}}} & -\alpha_2 e^{-\beta_2 d^{\mathtt{s}}} & \alpha_2 e^{\beta_2 d^{\mathtt{s}}} \\ -\gamma_1 e^{-\mathtt{i}\beta_1 d^{\mathtt{s}}} & \gamma_1 e^{\mathtt{i}\beta_1 d^{\mathtt{s}}} & -\gamma_2 e^{-\beta_2 d^{\mathtt{s}}} & \gamma_2 e^{\beta_2 d^{\mathtt{s}}} \end{bmatrix}, \tag{22}$$

$$\mathscr{A} = \begin{bmatrix} 1 & 1 & 1 & 1 \\ -\mathtt{i}\beta_1 & \mathtt{i}\beta_1 & -\beta_2 & \beta_2 \\ e^{-\mathtt{i}\beta_1 d^{\mathtt{s}}} & e^{\mathtt{i}\beta_1 d^{\mathtt{s}}} & e^{-\beta_2 d^{\mathtt{s}}} & e^{\beta_2 d^{\mathtt{s}}} \\ -\mathtt{i}\beta_1 e^{-\mathtt{i}\beta_1 d^{\mathtt{s}}} & \mathtt{i}\beta_1 e^{\mathtt{i}\beta_1 d^{\mathtt{s}}} & -\beta_2 e^{-\beta_2 d^{\mathtt{s}}} & \beta_2 e^{\beta_2 d^{\mathtt{s}}} \end{bmatrix}. \tag{23}$$

Here, α_1, α_2, γ_1 and γ_2 are four coefficients given by:

$$\alpha_1 = \mathtt{i}\beta_1^3 + \mathtt{i}\beta_y^2(2-\nu)\beta_1, \quad \alpha_2 = -\beta_2^3 + \beta_y^2(2-\nu)\beta_2, \quad \gamma_1 = \beta_1^2 + \nu\beta_y^2, \quad \gamma_2 = -\beta_2^2 + \nu\beta_y^2. \tag{24}$$

By considering the dynamic stiffness matrix $\mathbf{D}^{\mathtt{SE}}$ (Eq. (21)), the transfer matrix $\mathbf{S}$ of the strip can be derived (Goldstein *et al.*, 2010):

$$\mathbf{S} = \begin{bmatrix} -(\mathbf{D}^{\mathtt{SE}}_{\mathtt{LR}})^{-1}\mathbf{D}^{\mathtt{SE}}_{\mathtt{LL}} & (\mathbf{D}^{\mathtt{SE}}_{\mathtt{LR}})^{-1} \\ -\mathbf{D}^{\mathtt{SE}}_{\mathtt{RL}} + \mathbf{D}^{\mathtt{SE}}_{\mathtt{RR}}(\mathbf{D}^{\mathtt{SE}}_{\mathtt{LR}})^{-1}\mathbf{D}^{\mathtt{SE}}_{\mathtt{LL}} & -\mathbf{D}^{\mathtt{SE}}_{\mathtt{RR}}(\mathbf{D}^{\mathtt{SE}}_{\mathtt{LR}})^{-1} \end{bmatrix}. \tag{25}$$

The transfer matrix of a substructure, e.g., which is made up of three strips with different material properties ($\mathtt{Mat1} - \mathtt{Mat2} - \mathtt{Mat1}$), follows as:

$$\mathbf{S} = \mathbf{S}_{\mathtt{Mat1}}\mathbf{S}_{\mathtt{Mat2}}\mathbf{S}_{\mathtt{Mat1}}. \tag{26}$$

In the same way as for the WFE method, the eigensolutions of the transfer matrix $\mathbf{S}$ of the substructure (three strips) — say, $\mu_j^{\mathtt{SE}}$ — are calculated, which provides the wavenumbers $\beta_j^{\mathtt{SE}}$:

$$\beta_j^{\mathtt{SE}} = -\frac{\mathtt{ln}(\mu_j^{\mathtt{SE}})}{\mathtt{i}d}, \tag{27}$$

where $d = d_1^{\mathtt{s}} + d_2^{\mathtt{s}} + d_3^{\mathtt{s}}$ is the substructure length.

4. NUMERICAL RESULTS

Numerical simulations are carried out to illustrate the capability of the WFE method to calculate band gaps in PC plates and PC cylindrical shells with 1D periodic elastic properties (Figure 1). The structures under concern are made of strips with two different material properties. The dispersion curves issued from the WFE method are assessed and compared with the SE method (Section 3). Also, the vibration attenuation in the frequency response functions (FRFs) of the structures is analyzed.

4.1 Periodic plate

Consider a simply-supported plate made up of identical substructures which are meshed by means of 2D rectangular plate elements with four nodes and three DOFs per node (one displacement and two rotations). Two examples are proposed here to compare the WFE method with the SE method. The first example involves a homogeneous plate made of stainless steel; the second one concerns a plate with a periodic distribution of strips with two different material properties (see Figure 1), i.e., stainless steel and polyacetal. The choice of these materials is based on the differences between their elastic properties, which allows the formation of band gaps at low-and mid-frequencies. Those material properties are listed in Table 1.

Table 1: Material properties.

Material	Stainless Steel	Polyacetal
Young's modulus (GPa)	193	3.3
Density (kg/m^3)	8030	1418
Poisson ratio	0.27	0.35
Loss factor	0.001	0.001

The dispersion curves — i.e., the frequency evolution of the wavenumbers β_j — for the waves in the homogeneous plate are shown in Figure 2. The geometrical properties of the related substructure are: length of $d = 0.01$ m; width of $L_y = 0.2$ m and thickness of $h = 0.001$ m . The WFE solutions are plotted (solid lines) along with the SE solutions (circles). The imaginary values of the wavenumbers are represented as negative values (Doyle, 1997). It can be seen that the WFE solutions perfectly match the reference SE results, hence giving credit to the WFE method. To achieve the WFE modeling, attention has been paid on discretizing the substructure with a sufficient number of elements to accurately capture the analytical waves occurring in an equivalent infinite Kirchhoff-Love plate. This means eight elements per wavelength (at least). In this sense, the WFE method can be proven highly accurate to compute the waves in homogeneous plates, and more generally in periodic structures.

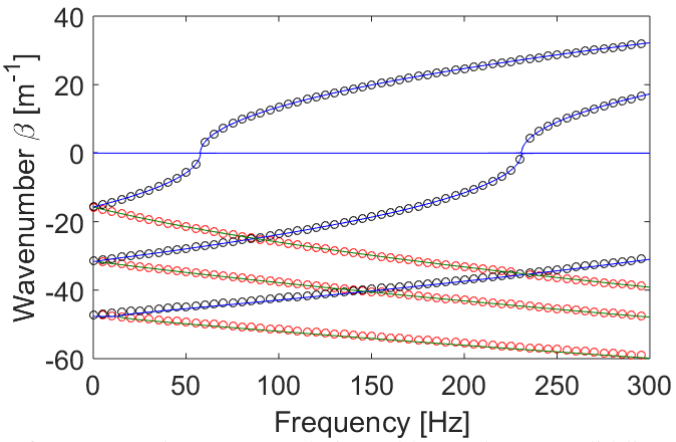

Figure 2: Dispersion curves for a Levy plate: WFE solutions (blue and green solid lines); SE solutions (black and red circles).

Consider now a PC plate that consists of a periodic distribution of strips with different material properties (two materials: stainless steel and polyacetal). The whole periodic structure is made up of $N = 4$ identical substructures with a length of $3d = 3 \times 0.1$ m as shown in Figure 3. The periodic structure is excited on its left side by means of a uniform distribution of transverse forces (Figure 3). Also, the magnitude of the transverse displacement is analyzed at one measurement point on the right side as shown (Figure 3). The FRF of the structure is computed over a frequency band of $\mathcal{B}_f = [0.2, 300]$ Hz along with the dispersion curves of the bending mode (Figure 4). Regarding the dispersion curves, both WFE and SE solutions are highlighted. Also, the Bragg limit is displayed which corresponds to the case $\beta_j = \pi/d = 10.47$ m^{-1}.

Figure 4 clearly highlights the influence of the periodic distribution of two materials on the formation of Bragg-type band gaps. These occur when the imaginary part of the wavenumber becomes negative (evanescent waves). These band gaps are mostly induced by Bragg scattering effect, which is due to the impedance mismatches between the strips. Again, the dispersion curves issued from the WFE method perfectly match the SE solutions over the whole frequency range. Also, the WFE method can be used to obtain the FRF of the periodic structure (Figure 4). It is seen that the vibration levels are well attenuated when band gaps occur, as expected.

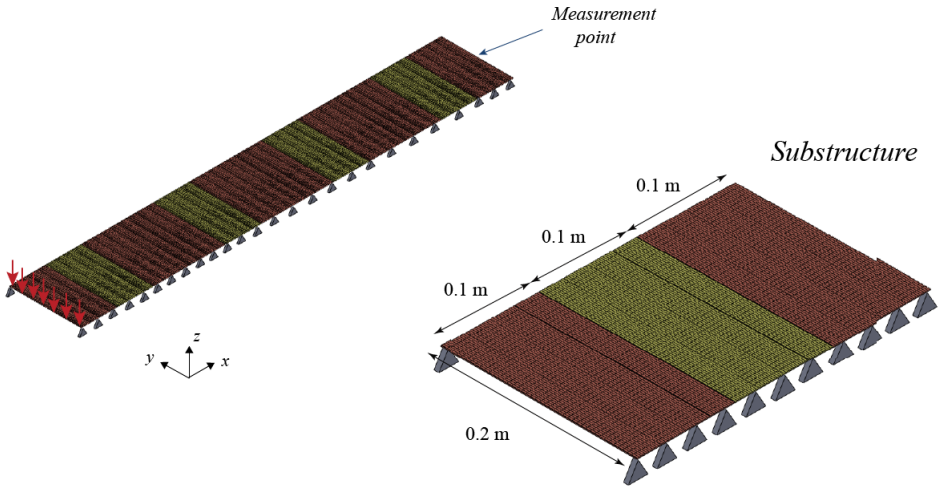

Figure 3: Periodic structure with $N = 4$ substructures (left), and FE mesh of a substructure (right).

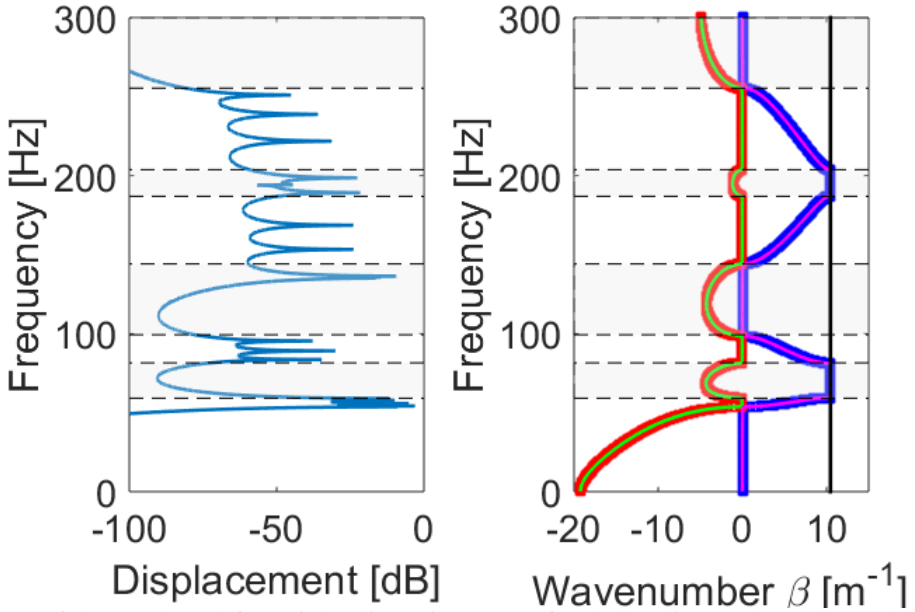

Figure 4: (Left) FRF of the PC plate (left); (Right) dispersion curves for the bending mode: real part (blue) and imaginary part (red) of the SE solution; real part (magenta) and imaginary part (green) of the WFE solution; Bragg limit (black line).

4.2 Periodic cylindrical shell

Consider now a cylindrical shell composed of identical substructures which are meshed with 2D rectangular thin flat shell elements with four nodes and six DOFs per node. First, a homogeneous cylindrical shell is analyzed which is made of stainless steel. The geometrical properties of a substructure are: length of $d = 0.05$ m, radius of $R = 0.05$ m and thickness of $h = 0.0025$ m. The dispersion curves of the structure are computed with the WFE method and compared to the Flügge shell theory (Liu *et al.*, 2009) (see Figure 5). Here, the parameters $\beta_j R$ are plotted as functions of the non-dimensional frequency $\Omega = \omega R/c_L$ where c_L is the longitudinal wave speed (Liu *et al.*, 2009). In this case again, it is seen that the WFE method is in perfect agreement with the analytical theory.

Consider now a PC cylindrical shell made up of $N = 20$ substructures as show in Figure 6. Each substructure is composed of two layers of stainless steel of length 0.01 m (red material) which surround one layer of polyacetal of length 0.03 m (yellow material). The whole periodic structure is excited by means of two radial point forces acting in opposite

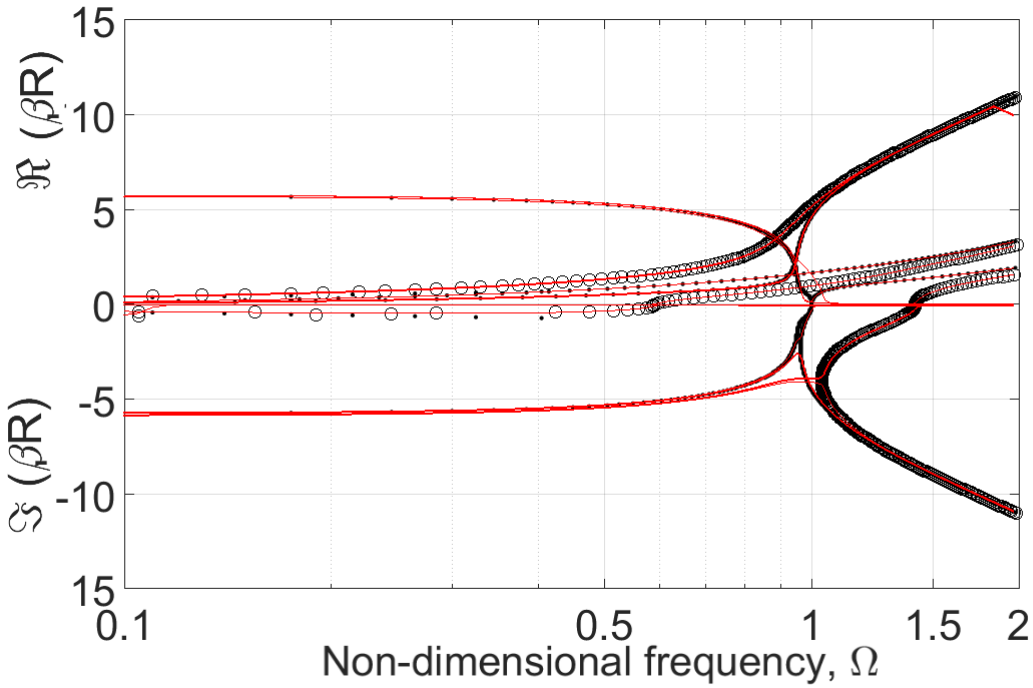

Figure 5: Dispersion curves for a homogeneous cylindrical shell: WFE solutions (red solid lines); analytical solutions (black dots and black circles).

directions on the left cross-section, while it is clamped on the right cross-section (see Figure 6). The magnitude of the vertical displacement (y- direction) is analyzed at one measurement point at the middle of the cylindrical shell as shown in Figure 6. The FRF of the structure is computed with the WFE method over a frequency band of $\mathcal{B}_f = [100, 20000]$ Hz along with the dispersion curves of two significant modes (Figure 7). In this case, the Bragg limit gives $\beta_j = \pi/d = 62.83$ m^{-1}. Here again, several bad gaps can be well predicted which agree with the frequency regions over which the vibration levels of the structure are attenuated (Figure 7).

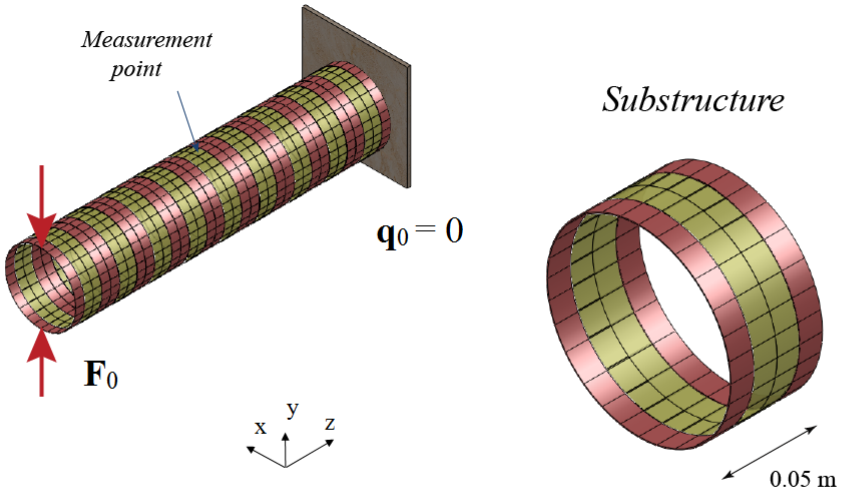

Figure 6: Periodic structure with 20 substructures (left), and FE mesh of a substructure (right).

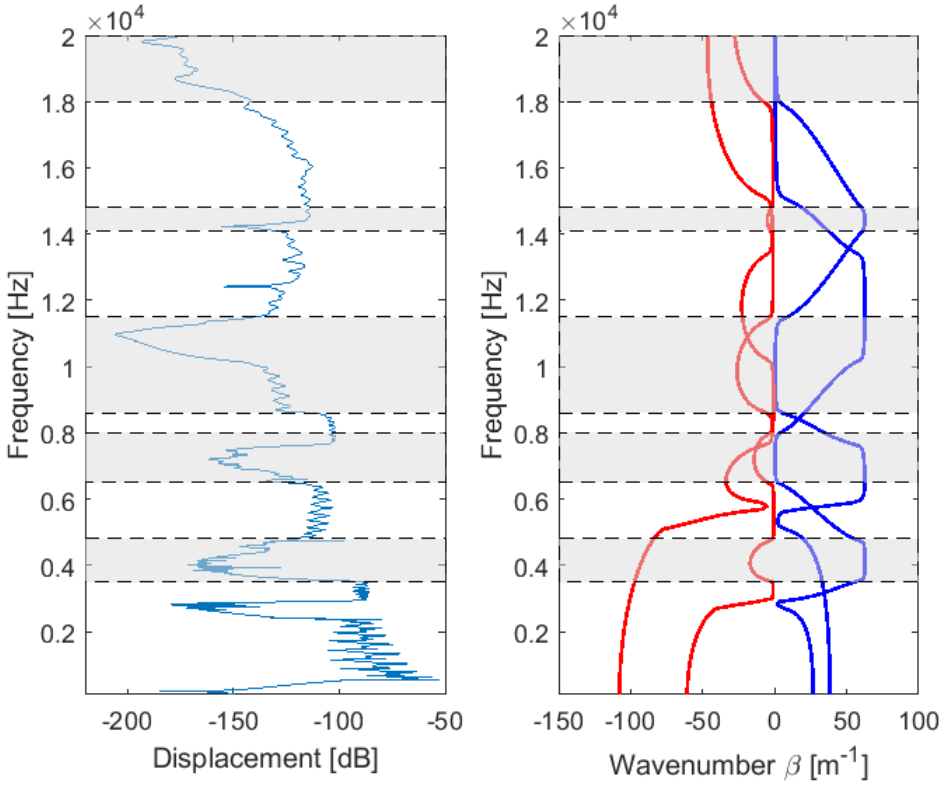

Figure 7: Frequency response of periodic PC cylindrical shell (left), and dispersion curves for two modes in the PC cylindrical shell (right). Real part (blue) and imaginary part (red) of the WFE solution.

5. CONCLUSION

The WFE method has been applied to analyze the wave propagation in plates and cylindrical shells with a periodic distribution of strips of different materials. The accuracy of the WFE method has been clearly demonstrated when compared to the analytical theories. Numerical experiments have been carried out which clearly highlight the relevance of the proposed approach for predicting band gaps in elastic PC structures. As it turns out, the WFE method appears to be an efficient numerical tool for predicting band gaps in periodic structures with complex periodicity patterns (shapes and material distributions). In particular, it could be applied to improve the design of periodic structures so as to magnify their band gap mechanisms.

6. REFERENCES

Arruda, J., Donadon, L., Nunes, R. and Albuquerque, E., 2004. "On the modeling of reinforced plates in the mid-frequency range". pp. 1407–1416.

Campos, N. and Dos Santos, J., 2015. "A Spectral Element Method Formulation for Rectangular thin Plates". *International Journal of Civil & Environmental Engineering*, Vol. 15, No. 2, pp. 38–44.

Doyle, J., 1997. *Wave Propagation in Structures: Spectral Analysis Using Fast Discrete Fourier Transforms*. Mechanical Engineering Series. Springer New York. ISBN 9780387949406.

Duhamel, D., Mace, B. and Brennan, M.J., 2006. "Finite element analysis of the vibrations of waveguides and periodic structures". *Journal of Sound and Vibration*, Vol. 294, No. 1-2, pp. 205–220.

Goldstein, A.L., Arruda, J.R.F., Silva, P.B. and Nascimento, R., 2010. "Building Spectral Element Dynamic Matrices Using Finite Element Models of Waveguide Slices". *Proceedings of ISMA2010 including USD2010,, Leuven, Belgium*, Vol. 20, pp. 2317–2330.

Hsu, J.C. and Wu, T.T., 2006. "Efficient formulation for band-structure calculations of two-dimensional phononic-crystal plates". Vol. 74.

Hussein, M., Leamy, M. and Ruzzene, M., 2014. "Dynamics of phononic materials and structures: Historical origins, recent progress, and future outlook". Vol. 66, p. 040802.

Lee, U. and Lee, J., 1999. "Spectral-element method for levy-type plates subject to dynamic loads". *Journal of Engineer-*

ing Mechanics, Vol. 125, No. 2, pp. 243–247.

Liu, Y.C., Hwang, Y.F. and Huang, J.H., 2009. "Modes of wave propagation and dispersion relations in a cylindrical shell". *Journal of Vibration and Acoustics, Transactions of the ASME*, Vol. 131, No. 4, pp. 0410111–0410119.

Mead, D., 1970. "'Free wave propagation in periodically supported, infinite beams'". *Journal of Sound and Vibration*, Vol. 11, No. 2, pp. 181 – 197. ISSN 0022-460X.

Mencik, J.M., 2014. "New advances in the forced response computation of periodic structures using the wave finite element (WFE) method". *Computational Mechanics*, Vol. 54, No. 3, pp. 789–801.

Mencik, J.M. and Duhamel, D., 2015. "A wave-based model reduction technique for the description of the dynamic behavior of periodic structures involving arbitrary-shaped substructures and large-sized finite element models". *Finite Elements in Analysis and Design*, Vol. 101, pp. 1–14.

Mencik, J.M. and Ichchou, M.N., 2005. "Multi-mode propagation and diffusion in structures through finite elements". *European Journal of Mechanics - A/Solids*, Vol. 24, No. 5, pp. 877–898.

Nobrega, E., Gautier, F., Pelat, A. and Dos Santos, J., 2016. "Vibration band gaps for elastic metamaterial rods using wave finite element method". *Mechanical Systems and Signal Processing*, Vol. 79, pp. 192–202.

Shen, H., Wen, J., Yu, D., Asgari, M. and Wen, X., 2013. "Control of sound and vibration of fluid-filled cylindrical shells via periodic design and active control". Vol. 332, pp. 4193–4209.

Sorokin, S. and Ershova, O., 2004. "Plane wave propagation and frequency band gaps in periodic plates and cylindrical shells with and without heavy fluid loading". Vol. 278, pp. 501–526.

Wu, T.T., Hsu, J.C. and Sun, J.H., 2011. "Phononic Plate Waves". *IEEE Transactions on Ultrasonics, Ferroelectrics and Frequency Control*, Vol. 58, No. 10, pp. 2146–2161.

7. ACKNOWLEDGEMENTS

The authors are thankful to the Program "Cátedras Francesas na UNICAMP" and Fundação de Apoio à Pesquisa do Estado do Maranhão (FAPEMA) for the financial support.

8. RESPONSIBILITY NOTICE

The following text, properly adapted to the number of authors, must be included in the last section of the paper:
The author(s) is (are) the only responsible for the printed material included in this paper.